

**Observation of Andreev bound states in
YBa₂Cu₃O_{7-x}/Au/Nb ramp-type Josephson junctions**

B. Chesca ^{1*}, D. Doenitz ¹, T. Dahm ², R. P. Huebener ¹, D. Koelle ¹, R. Kleiner ¹,
Ariando ³, H.J.H. Smilde ³, H. Hilgenkamp ³

*1: Physikalisches Institut-Experimentalphysik II, Universität Tübingen,
Auf der Morgenstelle 14, D-72076 Tübingen, Germany*

*2: Institut für Theoretische Physik, Universität Tübingen,
Auf der Morgenstelle 14, D-72076 Tübingen, Germany*

*3: Faculty of Science and Technology and Mesa⁺ Research Institute, University of Twente
P.O. Box 217, 7500 AE Enschede, The Netherlands*

We report on Josephson and quasiparticle tunneling in YBa₂Cu₃O_{7-x}(YBCO)/Au/Nb ramp junctions of several geometries. Macroscopically, tunneling occurs in the ab-plane of YBCO either in the (100) and (010) direction, or in the (110) direction. These junctions have a stable and macroscopically well defined geometry. This allows systematic investigations of both quasiparticle and Josephson tunneling over a wide range of temperature and magnetic field. With Nb superconducting, its gap appears in the quasiparticle conductance spectra as Nb coherence peaks and a dip at the center of a broadened zero-bias conductance peak (ZBCP). As we increase the temperature or an applied magnetic field both the Nb coherence peaks and the dip get suppressed and the ZBCP fully develops, while states are conserved. With Nb in the normal state the ZBCP is observed up to about 77 K and is almost unaffected by an increasing field up to 7 T. The measurements are consistent with a convolution of density of states with broadened Andreev bound states formed at the YBCO/Au/Nb junction interfaces. Since junctions with different geometries are fabricated on the same substrate under the same conditions one expects to extract reliable tunneling information that is crystallographic direction sensitive. In high contrast to Josephson tunneling, however, the quasiparticle conductance spectra are crystallographic orientation insensitive: independent whether the tunneling occurs in the (100) or (110) directions, a pronounced ZBCP is always observed, consistent with microscopic roughness of the junction interfaces. Furthermore we show that by increasing the Au gold layer thickness over a certain limit the ZBCP completely vanishes.

PACS: 74.20.Rp, 74.50.+r, 74.78.Bz.

I. INTRODUCTION

Quasiparticle tunneling spectroscopy has been accepted to be one of the most sensitive probes of electronic states of superconductors. The appearance of a zero-bias conductance peak (ZBCP) in the differential conductance $G = dI/dV$ versus voltage V , due to the formation of Andreev bound states (ABS) at interfaces involving $d_{x^2-y^2}$ (d)-wave superconductors is one of the most remarkable features distinct from conventional s -wave superconductors [1-6]. So far, ABS induced ZBCPs have been experimentally observed in three different systems: NIS_d, S_dIS_d, and S_dIS_s junctions, where N is a normal metal, I is an insulator, and S_d (S_s) is a d -wave (s -wave) superconductor. For NIS_d junctions the formation of ABS and its implication on tunneling spectra has been intensively investigated experimentally and is well understood theoretically [5,6]. In contrast S_dIS_d [8,9] and S_dIS_s [10-12] junctions have been much less investigated experimentally. These systems are of particular interest since both Cooper pairs and quasiparticles are tunneling simultaneously. Therefore a direct comparison between the two tunneling channels from the point of view of potential tools for investigating the symmetry of the order parameter [2, 6, 7] is possible, although, as far as S_dIS_s junctions are concerned

* Corresponding author: boris.chesca@uni-tuebingen.de

all reports [10-12] have concentrated on quasiparticle tunneling only. In addition, as shown in the pioneering theoretical work [4], the energy gap of the S_s superconductor appears on the conductance tunneling spectra of S_dIS_s junctions in the form of a center dip. Observation of such a center dip superposed on a broader ZBCP rules out all the other alternative mechanisms (like supercurrent leakage, tunneling into a normal region, or scattering due to magnetic impurities in the barrier) that may induce a ZBCP as well, and therefore unambiguously proves the existence of ABS [4]. This is an important advantage S_dIS_s have over S_dIN and S_dIS_d junctions that makes them very attractive tools to be used in phase-sensitive experiments to determine the symmetry of the superconducting order parameter. Finally, the striking similarity of the ZBCP in NIS_d and $S_dIS_{d,s}$ ($S_{d,s}$ means that the superconductor is either a d -wave or an s -wave superconductor; $S_d = YBa_2Cu_3O_{7-x}$ (YBCO) and $S_s = Nb$ in the case studied in this paper) systems is not well understood. There have been two scenarios proposed to explain such a similarity. Some authors consider that the ZBCP in the $G(V)$ characteristic of $S_dIS_{d,s}$ junctions results from a convolution of density of states with strongly broadened mid-gap-states [4,8,9]. Other authors proposed a different model [6, page R72]. In their view for an $S_dIS_{d,s}$ junction to behave like a NIS_d junction it is necessary that there are strong relaxation effects in the barrier region, the barrier acting as a reservoir, which results in decoupling of the two S_dI and $IS_{d,s}$ interfaces. The resulting system will then be a series connection $S_dI+IS_{d,s}$ of two independent junctions (here we call this model [6] the $S_dI+IS_{d,s}$ model). For identical transparencies each junction would be biased by $V/2$ and the s -wave gap should occur well above Δ_s/e . In contrast, in the frame of the $S_dIS_{d,s}$ convolution model the s -wave gap should occur at Δ_s/e and the d -wave gap appears at Δ_d/e . Since there has been no independent measurement of the gap in experiments involving such junctions so far it remained an open question which of the models is appropriate for $S_dIS_{d,s}$ junctions.

In order to gain knowledge and a deeper understanding concerning all these issues related to tunneling from one superconductor to another, in this work we present measurements of both Josephson and quasiparticle tunneling in $YBaCuO/Au/Nb$ ramp type junctions [13]. As it will be clear later on, the quasiparticle conductance measurements suggest the presence of a thin insulating tunnel barrier which develops at the YBCO/Au interface, so that S_dINS_s junctions are actually formed. Then, due to a proximity effect in the Au layer, such junctions behave like S_dIS_s junctions. The junctions investigated here have the advantage of being realized in a well controlled junction geometry, so that macroscopically tunneling can be probed in different directions. This important feature allows systematic investigations of both quasiparticle and Josephson tunneling over a wide range of temperature and magnetic field for junctions of different orientations fabricated on the same chip. The Josephson channel may be switched off by a small applied magnetic field. That opens a unique opportunity to directly compare the two tunneling channels as tools to investigate the junction structure and the symmetry of the superconducting order parameter [2,6,7]. We will show that both tunneling methods are actually complementary to one another. In particular we present evidence of Andreev bound states formation at the YBCO/Au interface independent on the macroscopic tunneling direction, i.e., for both (100) and (110) junctions. On the other hand, the junctions investigated here offer the unique opportunity to clarify the issue which of the models, the S_dIS_s convolution model or the S_dI+IS_s model, is appropriate for tunneling from one superconductor to another. This is possible since the gap of the S_s (Nb) is well defined and easy to interpret in the conductance spectra. Also the S_d (YBCO) gap is a reasonably well known quantity from various types of experiments.

The paper is structured as follows: in section II we present a representative selection of the measurements performed: current –voltage characteristics (IVCs), maximum Josephson critical current I_c versus small applied magnetic fields B (in the μT range) and quasiparticle tunneling spectra $G(V)$ for large applied magnetic fields (from 0.1 T up to 7 T) and variable temperature T (from 4.2 K up to 77 K), and for different Au barrier thickness. In section III we present theoretical approaches developed in an effort to explain both the Josephson and quasiparticle tunneling experimental data. Those calculations allow: a) to gain insights into the junction structure, in particular about the scattering rates at both YBCO/Au and Au/Nb interfaces and on the interface roughness, and b) to distinguish between the S_dIS_d convolution model and the $S_dI+IS_{d,s}$ model.

II. TUNNELING EXPERIMENTS IN YBCO/AU/NB JUNCTIONS

For the experiments YBCO/Au/Nb ramp junctions of several geometries were used, see Fig.1. Macroscopically, tunneling occurs in either the (100) direction, or the (110)

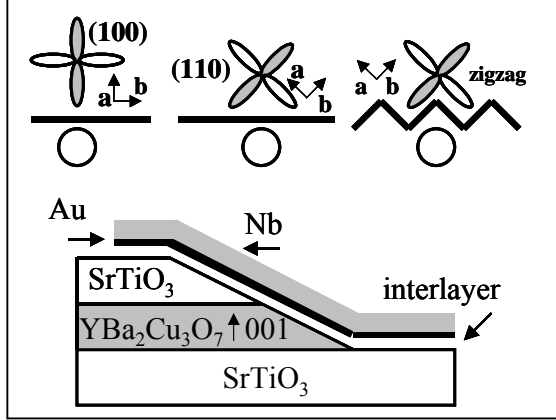


FIGURE 1: Schematic topview of a (100), a (110), and a zigzag junction and a sideview of a $\text{YBa}_2\text{Cu}_3\text{O}_{7-x}$ /Au/Nb ramp-type junction.

direction, or both (100) and (010) directions simultaneously. The directions are taken with respect to the YBCO crystallographic orientations. Following notations from [13] we call the latter type of junctions having N number of alternating (100) and (010) facets, zigzag junctions. It is important to note that the films used in these experiments are twinned. That means that in the case of a (100) or (010) facet there is always a combination of (100) and (010) tunneling directions. However, in the following, we will refer to (100) and (010) in the macroscopic tunneling directions simply to indicate a 90° difference in the tunneling directions with respect to a fixed orientation in the ab plane of the substrate. Fabrication [13] of these junctions as well as Josephson tunneling in these systems [14] have been reported elsewhere. We made four-point measurements in a liquid-helium cryostat ($T = 4.2$ K) to obtain the IVCs. Families of IVCs taken at various B values in an electrically shielded room and a magnetically well-shielded liquid-helium cryostat have been used to extract the $I_c(B)$ characteristics. The magnetic field was always applied along the (001) direction, i.e., perpendicular to the ab plane of YBCO. As far as quasiparticle spectra are concerned we numerically differentiate the IVCs to obtain the differential conductance. In total we measured 3 chips. Each chip contained 7 junctions with different geometries. Each chip is characterized by a different Au barrier thickness: 50 nm, 100 nm, and 150 nm, respectively. All of the experimental data presented except those from Fig.7 are for the junctions with a 100 nm Au barrier thickness. To make a selection, here we show measurements of a 50 μm wide (100) junction, a 280 μm wide (110) junction and 3 zigzag junctions: a junction with 10 facets of 40 μm (called 10 x 40 μm), a 40 x 5 μm junction, and a 8 x 25 μm junction.

A. JOSEPHSON TUNNELING

In accordance with earlier reports [14] for similar (100) and zigzag junctions, all junctions we measured at $T = 4.2$ K and zero applied magnetic field have hysteretic IVCs (see the inset of Fig.2b), that are well described by the resistively and capacitively shunted-junction (RCSJ) model [15]. We measured $I_c(B)$ as a function of small applied fields B in the μT range. At fields in the mT range or higher there is no trace of a Josephson supercurrent left on the IVC. The (100) junctions have an $I_c(B)$ that qualitatively resembles a Fraunhofer pattern (see Fig.2(a); also [14]). For the (110) junction the $I_c(B)$ pattern (see Fig.2(b)) is *qualitatively* different and consists of many peaks with amplitudes randomly distributed, similar to the case of 45° asymmetric bicrystal grain boundary junctions [16]. Such a pattern is clearly supportive of the d -wave symmetry of the superconducting order parameter in YBCO. It may be well understood qualitatively in terms of a junction interface that consists of a multitude of small junctions with positive and negative junction critical current densities [16,17]. For

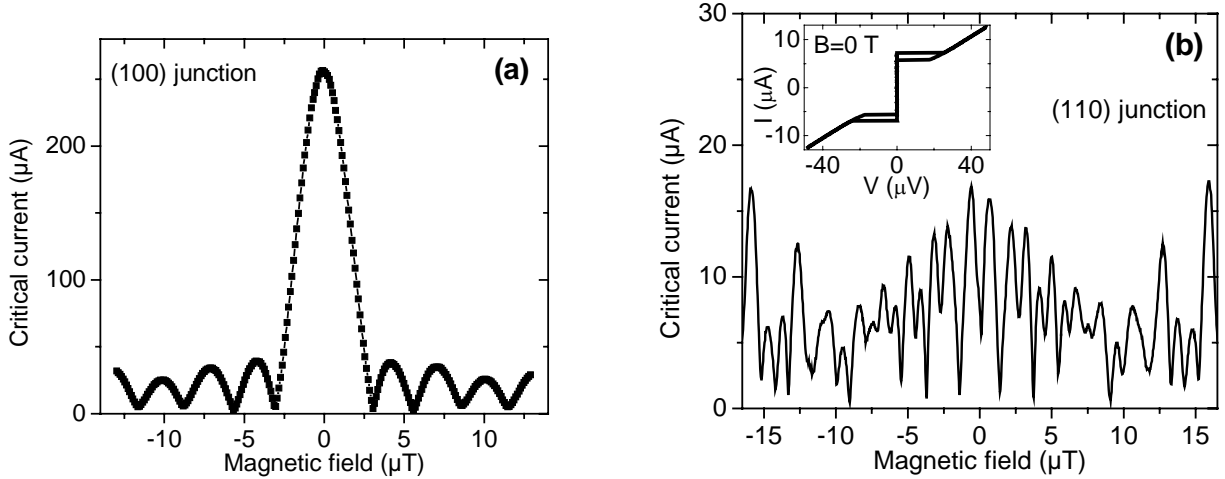


FIGURE 2: Critical current versus magnetic field measured at 4.2 K for (a) the (100) junction, and (b) the (110) junction. Inset in (b) show current-voltage characteristics (IVC) at $B=0$.

the zigzag junctions the $I_c(B)$ patterns (not shown here) are also anomalous with respect to the Fraunhofer pattern, similar to previous reports on similar junctions [14]. To conclude, Josephson tunneling is crystallographic orientation *sensitive*: there are sharp qualitative differences between various tunneling orientations.

B. QUASIPARTICLE TUNNELING

Figure 3 shows representative quasiparticle tunneling data at $B=0.01$ T of the (100) junction, the (110) junction, and of two zigzag junctions ($10 \times 40 \mu\text{m}$ and $40 \times 10 \mu\text{m}$), at two different temperatures: 4.2 K and 9.05 K (just below the critical temperature of Nb, $T_{c,\text{Nb}} \approx 9.1$ K). At 4.2 K pronounced gap-like features are observed at $V = \pm 1.5$ mV, in accordance with published values of the Nb energy gap. These data are very similar to other reported measurements in tunnel YBCO-Nb junctions [10]. At 9.05 K the Nb coherence peaks are completely suppressed and a pronounced ZBCP appears. In some cases (see for instance the $10 \times 40 \mu\text{m}$ zigzag junction shown again in Fig. 4a for larger voltages) a clear gap like feature is observed at about ± 19 mV that agrees well with other reported values in the literature for the YBCO gap [11,12].

We next discuss the B and T dependencies of the conductance spectra. Before we get into details, let us summarize some of the main results (cf. Figs. 4 and 5).

- a) As we increase T from 4.2 K up to slightly below $T_{c,\text{Nb}}$, or B from 0.1 T up to slightly below the second critical field of Nb ($B_{c,\text{Nb}} \approx 1.15$ T), we do observe one and the same qualitative picture which is *independent* of the crystallographic orientation. In other words, quasiparticle tunneling in (100), (110), or zigzag junctions look all alike.
- b) As superconductivity gets suppressed in Nb, by increasing T or B the Nb coherence peaks get suppressed and the ZBCP gradually develops. Close to the critical values ($T_{c,\text{Nb}}$ or $B_{c,\text{Nb}}$) of Nb there is no trace left of the Nb coherence peaks, while the ZBCP is fully developed.
- c) Increasing T or B slightly above the critical values, there is a clear relatively sudden vertical shift of the conductance spectra to lower values of $G(V)$. These shifts are due to the fact that now we measure the YBCO-I-Au junction resistance in series with the normal Nb layer. The degree of this sudden vertical shift of the conductance spectra varies from junction to junction and depends on the magnitude of the Nb normal resistance relative to the junction YBCO-I-Au resistance.
- d) Increasing T or B even further (from above $T_{c,\text{Nb}}$ up to 77 K, or from above $B_{c,\text{Nb}}$ up to 7 T), however, a significant difference appears between the T and B dependence of $G(V)$. The

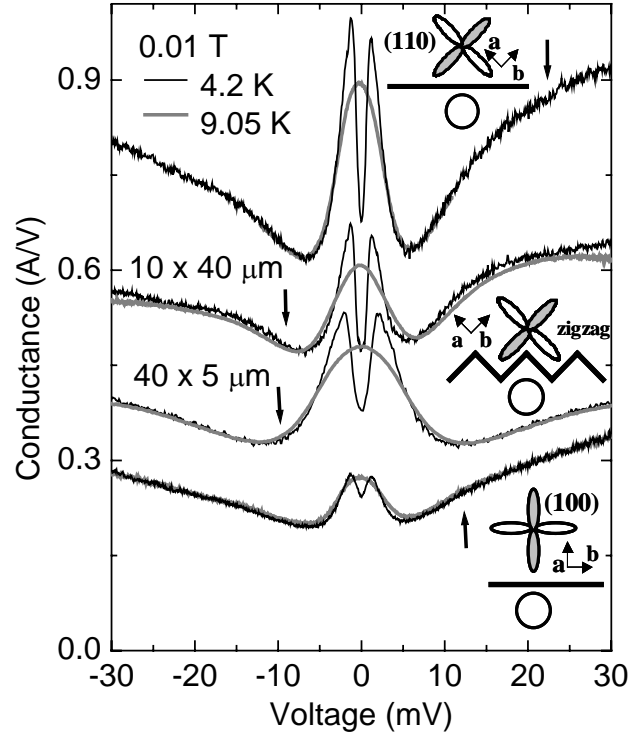


FIGURE 3: Tunneling spectra of 4 junctions having different geometries (see insets): the (100) and the (110) junctions, and the $10 \times 40 \mu\text{m}$ and $40 \times 5 \mu\text{m}$ zigzag junctions measured at two different temperatures: 4.2 K – thick line, and 9.05 K (just below $T_{c,\text{Nb}}$) – thin line. A magnetic field $B=0.01\text{ T}$ has been applied to completely suppress the Josephson critical current.

ZBCP (its amplitude and width) is essentially not affected by an increase of B , while by increasing T the ZBCP gets strongly suppressed and it widens. In particular, at 77 K we could not observe any trace of a ZBCP. In addition, by increasing T or B the conductance spectra are gradually shifted vertically to lower values due to the field and temperature dependence of the conductance of the Nb normal layer.

Figure 4(a) shows the B dependence of $G(V)$ of a $10 \times 40 \mu\text{m}$ zigzag junction from 0.01 T up to $B_{c,\text{Nb}}$ at 4.2 K. In this case the YBCO coherence peaks are clearly seen at about $\pm 19 \text{ mV}$. The Nb

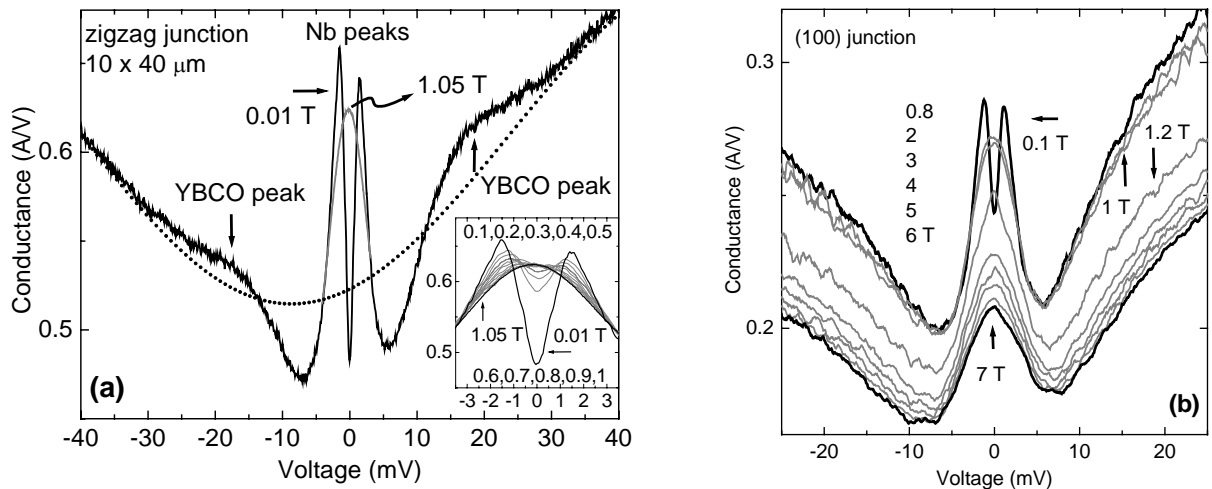


FIGURE 4: Tunneling spectra for different magnetic fields measured at 4.2 K. (a) $10 \times 40 \mu\text{m}$ zigzag junction (shown also in Fig.3) for $B = 0.01\text{ T}$ – in black, and $B = 1.05\text{ T}$ (just below $B_{c,\text{Nb}}$) – in gray. Dotted line shows the background conductance. The inset shows the low voltage conductance spectra at 11 different field values. (b) (100) junction for ten different B values from 0.1 T up to 7 T;

coherence peaks are gradually suppressed by an increasing field up to 1.05 T, as shown in the inset. Figure 4(b) shows 4.2 K conductance spectra of the (100) junction for 10 different values of B between 0.1 T and 7 T. Close to $B_{c,Nb} \approx 1.15$ T, there is no trace left of the Nb coherence peaks, while the ZBCP is fully developed. As explained before, increasing B further, there is a significant sudden vertical shift of conductivity at $B_{c,Nb}$ (compare the curves for 1 T and 1.2 T). Increasing B further, over $B_{c,Nb}$, up to 7 T the ZBCP is practically unaffected.

Figure 5(a) shows low voltage conductance spectra of a $40 \times 5 \mu\text{m}$ zigzag junction for 10 different temperatures between 4.2 K and $T_{c,Nb}$. As superconductivity gets suppressed in Nb, by increasing temperature T the Nb coherence peaks get suppressed too and the ZBCP gradually develops. Figure 5(b) shows the conductance spectra of the $8 \times 25 \mu\text{m}$ zigzag junction for 11 different temperatures between 4.2 K and 77 K. For this particular junction the vertical shift of the spectra induced by the Nb transition from its superconducting state to its normal state (see Fig.5(b), upper graph) is more pronounced than e.g. for the (100) junction. In addition, at the transition the ZBCP widens and its amplitude gets suppressed. Increasing T further over $T_{c,Nb}$ the ZBCP is gradually suppressed and is not visible anymore at 77 K (see Fig.5(b), lower graph).

In both situations (by increasing either T or H) the total number of states between -3 mV and 3 mV was conserved to a remarkable degree: to within 95 %, supporting the interpretation of the

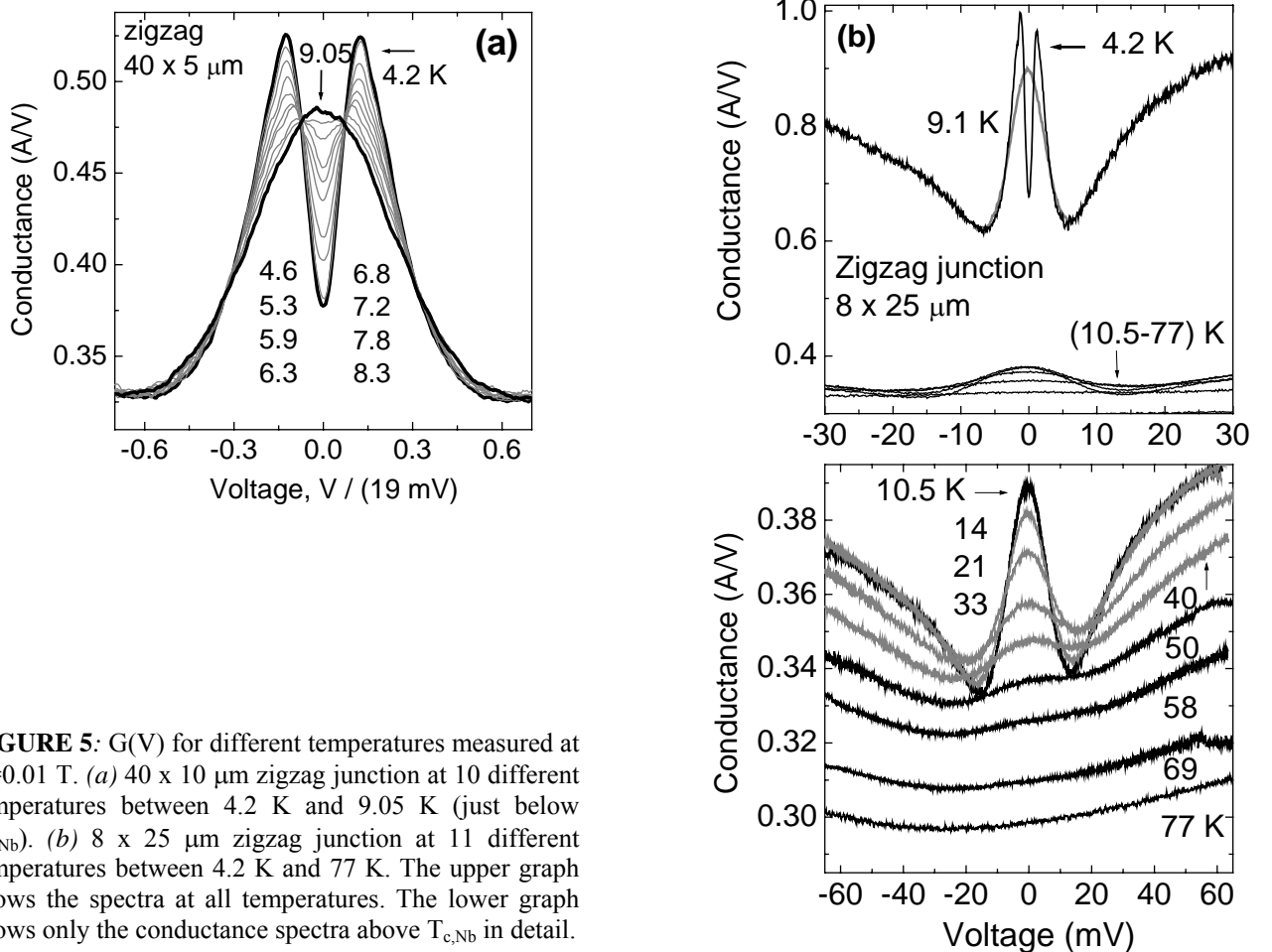
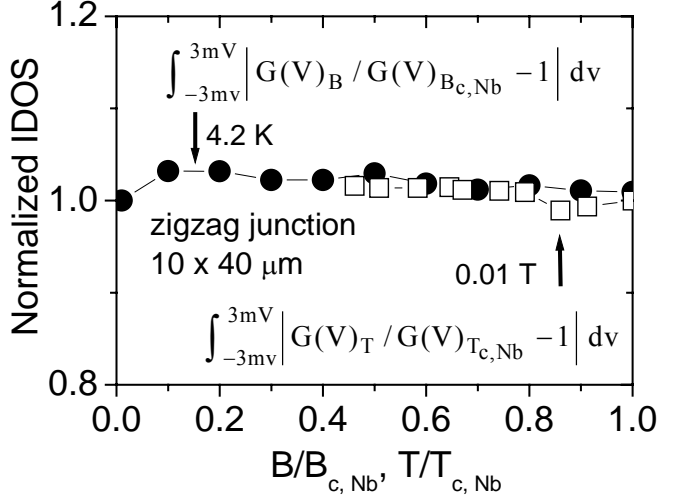


FIGURE 5: $G(V)$ for different temperatures measured at $B=0.01$ T. (a) $40 \times 10 \mu\text{m}$ zigzag junction at 10 different temperatures between 4.2 K and 9.05 K (just below $T_{c,Nb}$). (b) $8 \times 25 \mu\text{m}$ zigzag junction at 11 different temperatures between 4.2 K and 77 K. The upper graph shows the spectra at all temperatures. The lower graph shows only the conductance spectra above $T_{c,Nb}$ in detail.

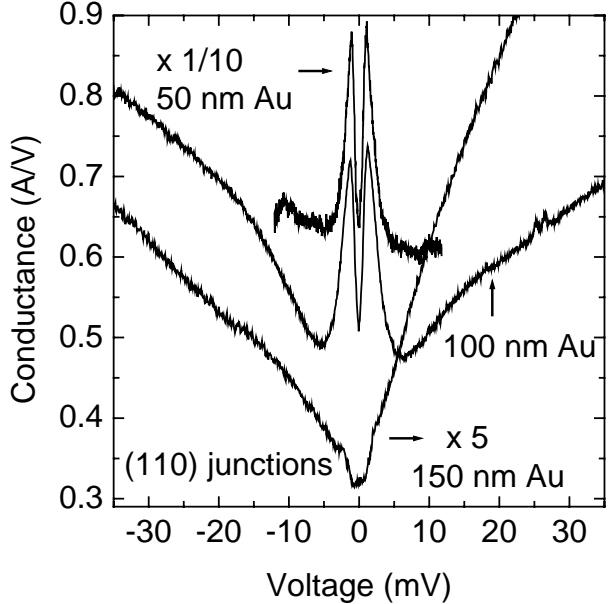
conductivity as a feature of a superconducting density of states. We have checked that precisely with similar results for many junctions by integrating the conductance spectra. One characteristic example is shown in Fig.6 for the zigzag junction 10×40 .

FIGURE 6: Normalized integrated density of states IDOS (between -3 mV and 3 mV) as a function of the normalized applied field B changed between 0.01 T and $B_{c2, Nb} \approx 1.1$ T (black circles) and the normalized temperature T changed between 4.2 K and $T_{c, Nb} \approx 9.1$ K (empty squares). $G(V)$ measurements versus T were made at 0.01 T, while $G(V)$ measurements versus B were made at 4.2 K.



The tunneling spectra exhibit a *qualitative* change when the Au barrier is changed from 100 nm to 150 nm. A representative example is shown in Fig. 7 for 280 μ m wide (110) junctions with different Au barrier thickness measured at 4.2 K and $B = 0.01$ T. Instead of a ZBCP, a conductance dip is observed at zero bias, while a gaplike feature cannot be resolved for the junction with a 150 nm thick Au barrier. Similar observations were made for all the other junction geometries as well. This suggests

FIGURE 7: $G(V)$ tunneling spectra at $T=4.2$ K and $B=0.01$ T of (110) junctions for different thickness of the Au barrier: 50 nm, 100 nm, and 150 nm. To facilitate the comparison between the different cases we have multiplied by 5 (divided by 10) the conductance spectra of the 150 nm (50 nm) thick Au barrier junction.



that a thick Au barrier is suppressing the formation of Andreev bound states, indicating that there is a maximal barrier thickness of a normal metal in S_d INS_s junctions for which the constructive interference producing a ZBCP occurs. Thus, for those thick Au barrier junctions the quasiparticle tunneling channel loses the signature of the d -wave symmetry of the order parameter. In contrast, the Josephson tunneling channel although strongly suppressed as well, does not. This is case since the $I_c(B)$ pattern of (110) junctions preserve its highly anomalous nature independent on the Au barrier thickness. Those observations suggest that a thicker junction barrier may completely suppress the ZBCP, but that fact should *not* be taken as evidence for an s -wave symmetry. This is consistent with a

recently suggested hypothesis concerning the first observation of a ZBCP in electron doped cuprate bicrystal grain boundary Josephson junctions (GBJs) [9]. In that work it was suggested that a ZBCP is much more difficult to observe in electron doped GBJs that are characterized by a much lower Josephson critical current density as compared to hole doped GBJs.

III. MODELING OF JOSEPHSON AND QUASIPARTICLE TUNNELING.

In qualitative agreement with calculations made for S_dIS_s tunneling junctions [4] the energy gap of the S_s superconductor (Nb) appears in our $G(V)$ measurements at 4.2 K in the form of a center dip (see Figs.3, 4, 5, and 7) whose magnitude is determined by the spectral weight of the zero-energy states due to the d -wave character of the S_d superconductor (YBCO). That indicates that tunneling largely contributes to the observed current in the junctions investigated here. It also suggests that the proximity effect induces superconductivity in the Au layer and consequently the junctions behave like S_dIS_s junctions. However, there are important quantitative discrepancies between calculations from [4] and our measurements that we address here. In particular, in our case the ZBCP is much more pronounced, and the zero bias conductance (ZBC), i.e., $G(V=0)$, below and above the critical temperature of the S_s superconductor is comparable to the conductance at the gap voltage $\Delta_d \approx 19$ mV of the S_d superconductor, and thus much larger than $G(V=0)$ calculated in [4].

To obtain a quantitative comparison with the measurements we have calculated the low transmission tunneling conductance of an S_dIS_s junction in the absence of an applied field using quasiclassical techniques as described in [18,19]. In this case the normalized conductance is given by

$$\frac{G(V)}{G_n} = \frac{1}{G_n} \frac{dI}{dV} = \frac{d}{dV} \int_{-\infty}^{\infty} dE N^d(E) N^s(E+V) [f(E) - f(E+V)] \quad (1).$$

Here $f(E) = 1/(1+\exp(E/k_B T))$ is the Fermi distribution function. $N^d(E)$ and $N^s(E)$ are the (normalized) local densities of states in the superconducting state on the d -wave and s -wave side, respectively. G_n and is the normal state conductance. On the s -wave side we take an s -wave density of states with a broadening parameter Γ_s and a gap value Δ_s with a BCS temperature dependence:

$$N^s(E) = \text{Re} \left[\frac{E + i\Gamma_s}{\sqrt{(E + i\Gamma_s)^2 + \Delta_s^2}} \right]$$

How can one understand the crystallographic orientation *insensitivity* of quasiparticle spectra in the frame of the rough interface junction model? In other words, no matter whether tunneling occurs in the (100), (110) or both (100) and (010) directions simultaneously, with Nb superconducting the two coherence peak structure is always present, while with Nb in the normal state a pronounced ZBCP is always observed (see Fig.3). Indeed, for perfectly smooth interfaces no ZBCP is expected for (100) junctions, or for zigzag junctions, while the ZBCP should reach its maximum in the case of (110) junctions. That strongly contradicts our observations. We argue here that it is the interface roughness that is responsible for this. In the case of NIS_d junctions it has been shown [3, 18, 19] that even a weak interface roughness or/and faceting both induce strong similarities between conductance spectra of (100) and (110) junctions. To get a good agreement with the experimental observations we have extended the rough interface junction model to S_dIS_s systems so that the calculated conductance spectra consequently will be crystallographic orientation *insensitive*. The roughness at the junction interface will smear out the uniqueness of the *macroscopic* tunneling orientation. Thus, on the d -wave side we average the surface local density of states over all possible angles of the surface with the orientation of the d -wave gap, in order to model the microscopic roughness of the junction. This gives the expression:

$$N^d(E) = \frac{2}{\pi^2} \int_{-\pi/4}^{\pi/4} d\varphi \int_{-\pi/2}^{\pi/2} d\theta \operatorname{Re} \left[\frac{E_+ E_- - \Delta_+ \Delta_-}{E_+ E_- + \Delta_+ \Delta_-} \right]$$

where $\Delta_{\pm} = \Delta_d \sin(2\theta \pm 2\varphi)$ and $E_{\pm} = E + i\Gamma_d + \sqrt{(E + i\Gamma_d)^2 + \Delta_{\pm}^2}$. Here, Δ_s and Δ_d are the gaps of the s -wave and d -wave superconductors, respectively, and Γ_d is a corresponding broadening parameter for the d -wave superconductor. In the inset of Fig. 8 we show $N^d(E)$ for different values of $\Gamma_d/\Delta_d = 0.15, 0.3$ and 0.6 , and $\Delta_s = 0.07\Delta_d$. Some results for the tunneling conductance Eq. (1) are shown in Fig. 8 for $T/T_{c,s} = 0.5$ and 1 , and different values of Γ_d . Here, $T_{c,s}$ is the critical temperature of the s -wave side. We have chosen $\Delta_s = 0.07\Delta_d$ and $\Gamma_s/\Delta_d = 0.05$, which gives the best fits to the experimentally observed s -wave peak structures. The ZBCP is strongly suppressed, and the ZBC strongly decreases with increasing broadening parameter Γ_d . The non-zero values for Γ_d and Γ_s naturally explain, in particular, why in our case, as well as, in [10] the ZBC is considerably larger than observed in other systems [11-12] and as predicted in [4].

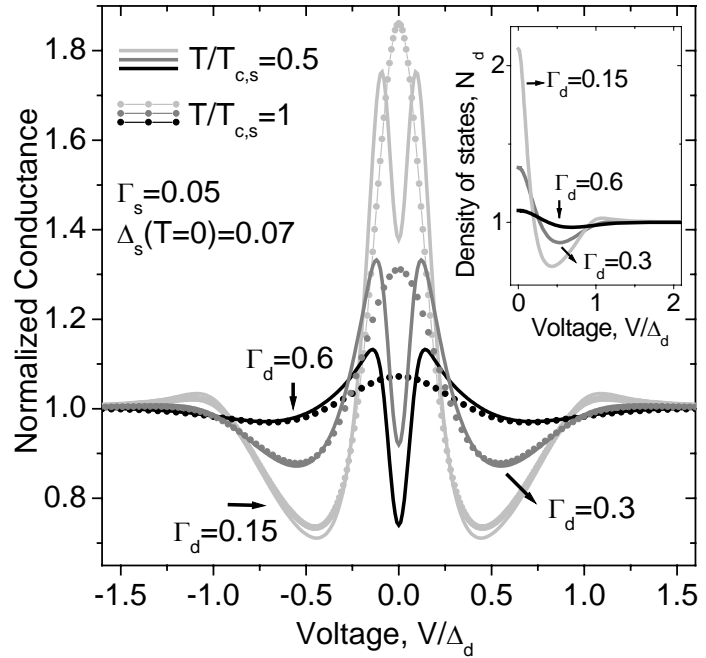


FIGURE 8: Calculated normalized $G(V)/G_N(V)$ spectra for two temperatures and three different values of the zero energy quasiparticle damping rate Γ_d at the YBCO d -wave superconductor interface in the frame of the S_dIS_s model. The inset shows the density of states in the d -wave superconductor (YBCO). Γ_d , Γ_s , Δ_s values are normalized to $\Delta_d = 1$.

On the other hand, how can we understand the $I_c(B)$ measurements that are strongly crystallographic orientation *sensitive* in the frame of the rough interface junction model? To answer this question we have calculated the $I_c(B)$ pattern for both (110) (Fig. 9a) and (100) junctions (Fig. 9b) according to the formula [20]:

$$I_c(B) = \int_{-\infty}^{+\infty} |J_c(x)e^{2\pi dixB/\Phi_0}| dx \quad (2)$$

Here $d = \lambda_{Nb} + \lambda_{YBCO} + t$, with t being the physical barrier thickness, and λ_{Nb} (λ_{YBCO}) the London penetration depth in Nb (YBCO). From Eq. (2) it follows that $I_c(B)$ is the modulus of the Fourier transform of the critical current density $J_c(x)$ profile along the junction width L , with $0 < x < L$. That means very accurate solutions for $J_c(x)$ at very small length scale (nm range) may only be tested for $I_c(B)$ measurements performed up to infinitely large magnetic fields. This is an impossible task in practice. Our primary goal therefore is not to obtain a very good quantitative agreement with the measurements but to show that a model of rough junctions, that comes out from quasiparticle

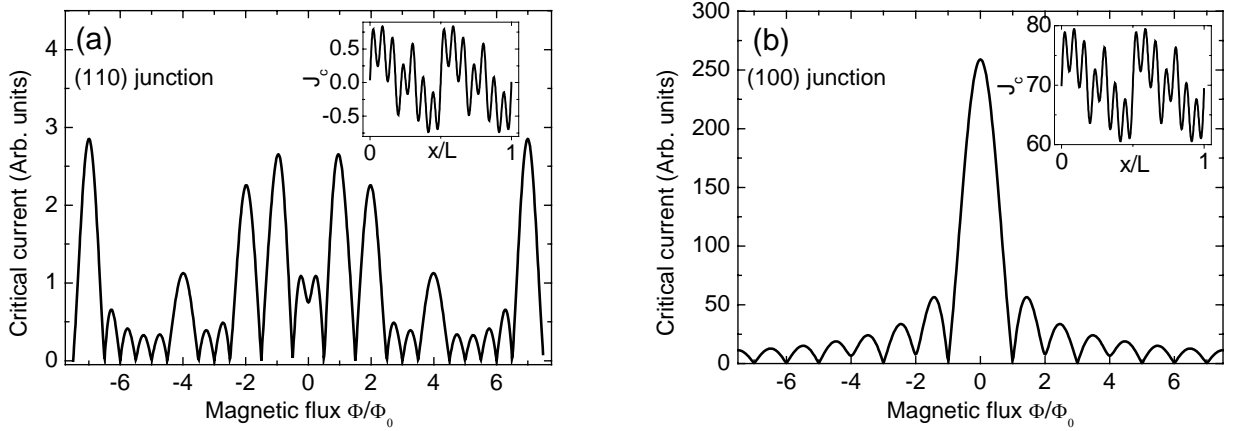


FIGURE 9: $I_c(B)$ patterns calculated with Eq.(2) for (a) a (100) and (b) a (110) Josephson junction formed between d -wave superconductors. We assume a J_c profile along the junction width L as shown in the insets. For the (100) junction the J_c profile is similar to the case of the (110) junction but multiplied by 10 and shifted vertically by 16.5 so that only positive values for the J_c are present.

tunneling, is consistent with the Josephson measurements as well (see Fig.2). In our model the tunneling orientation deviates locally from the macroscopic one and consequently is a function of coordinate x . Assuming YBCO has a d -wave symmetry of the order parameter it means J_c is a function of x , too. We therefore model the junction roughness as a *continuous* variation of $J_c(x)$ [21]. The tunneling direction deviations induce a significant change in the amplitude of $J_c(x)$ only on a scale that is about 2 orders of magnitude smaller than the junction widths. We do not exclude that significant changes of $J_c(x)$ may actually occur at a smaller scale too, but the signature of that would not appear on the $I_c(B)$ measurements we performed at small fields. For consistency, we assume a *similar* x -dependent $J_c(x)$ profile for both (100) and (110) junctions (see insets of Figs.9(a) and 9(b)). Thus, for the (110) junction $J_c(x)$ oscillates randomly between -0.7 and 0.82 (in arbitrary units) around the average value $\langle J_c(x) \rangle = 0.06$. For the (100) junction it oscillates *alike* between 60 and 80 units around the average value $\langle J_c(x) \rangle = 70$. The difference in $\langle J_c(x) \rangle$ between (110) and (100) junctions is due to the d -wave symmetry model of the order parameter in which J_c is a strongly angle dependent function and is expected to be zero if tunneling occurs *exactly* into the (110) direction and to have a certain maximum value for tunneling into the (100) direction. A reasonable qualitative agreement with the experiments (see Fig.2) is found as far as the essential features of the $I_c(B)$ patterns are concerned. For the (100) junction (see Fig.9(b)) one has a strong central maximum at $B=0$, followed by symmetrically distributed significantly smaller peaks. For the (110) junction one has a non-zero minimum at $B=0$, followed by a series of symmetrically distributed maxima characterized by amplitudes that differ randomly from one another. The huge difference in the maximum $I_c(B)$ values between the (100) and the (110) junctions (observed in the experiments, and confirmed by our calculations) can therefore be understood in terms of the (110) junction consisting of alternating regions with positive and negative junction critical current densities (see inset of Fig.9(a)). We simulated many other $J_c(x)$ profiles for both (100) and (110) junctions and compared them with the measurements. Here are some of the conclusions. Josephson tunneling measurements may provide a characteristic scale for the junction roughness. We found an upper limit of about a few hundreds of nm for significant non-uniformities in $J_c(x)$ of (100) junctions that are induced by the junction roughness. For (110) junctions we found that there must be significant $J_c(x)$ non-uniformities at a scale of about 10 μm . In addition, we cannot rule out that there might be significant $J_c(x)$ non-uniformities at a much smaller scale (nm scale), too. Moreover, this is most probably the case, since we needed to average over all possible tunneling

directions (from 0^0 up to 180^0) in the quasiparticle calculations in order to find a good agreement with the measurements.

Another interesting question we are able to answer is which of the two models for tunneling from a d -wave superconductor into an s -wave one is appropriate in our case: the S_dIS_s convolution model or the series connection S_dI+IS_s model [6, page R72] ? A significant difference is found between the two models in the location of the S_d and S_s coherence peaks which allows us a direct comparison with the measurements. The coherence peaks in the measured conductance spectra occur (see Figs.3, 4, and 5) at about the gap voltages of S_d (of about ± 19 mV for YBCO [10-11]) and S_s (of about ± 1.5 mV for Nb) in the S_dIS_s model. On the other hand, for the S_dI+IS_s model the coherence peaks occur essentially at *larger* values to a degree that depends on the relative conductances of S_dI and IS_s interfaces. For instance, for equal conductances of the two interfaces the coherence peaks occur at about double those values [6], while for the S_dI interface having much smaller conductance than the IS_s interface, the Nb coherence peak occur at a much larger value than ± 1.5 mV. In the experiments, however, we have clearly observed coherence peaks located at about ± 19 mV (for some junctions the YBCO peaks are less evident like in Fig.5b-upper graph, for others they are better pronounced –see Fig.4a) and ± 1.5 mV in all of the junctions measured which strongly suggests the S_dIS_s convolution model is appropriate in our case.

To perform a quantitative comparison of measured spectra with theory the experimental data have to be normalized to the normal-state background conductance. Experimentally we first have to increase temperature or magnetic field just over their critical values T_c and B_{c2} to suppress the superconductivity in the S_d superconductor, and then measure the normal-state background conductance. The problem is that B_{c2} of YBCO is difficult to reach in the experiments, while the normal-state background conductance may well be temperature dependent [2,6,12]. This is a serious complication that may distort the data and introduce significant errors [12]. To avoid these difficulties we normalize the measured spectra shown in Fig.5a to the curve at the critical temperature of Nb instead, as shown in Fig.10(a). Theoretically we first vary Γ_d , until the best fit is found of the measured

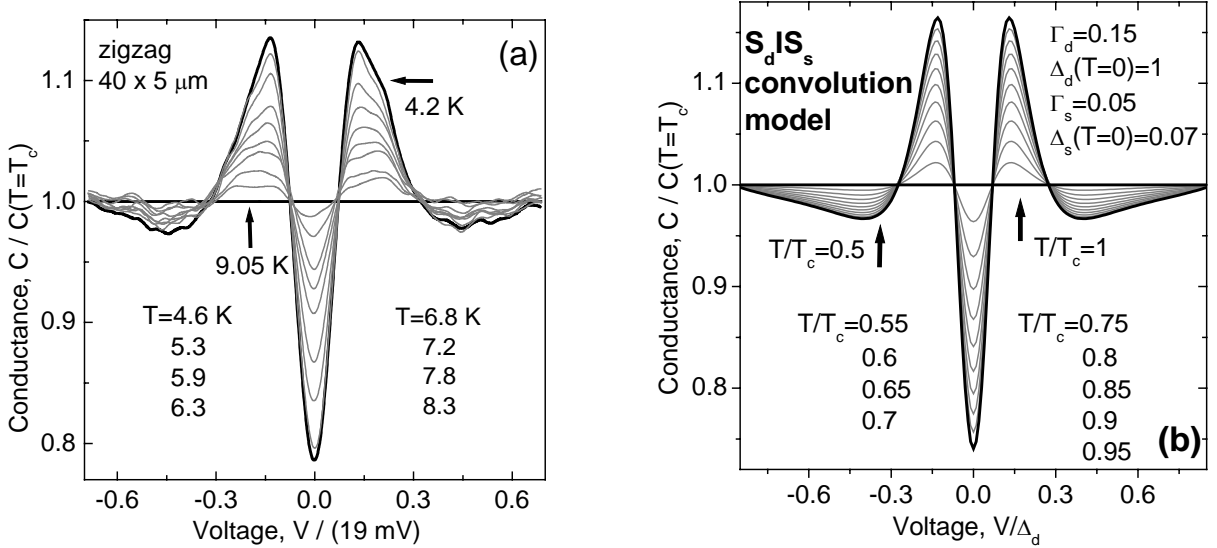


FIGURE 10: Normalized conductance spectra (a) of the $40 \times 5 \mu\text{m}$ zigzag junction (shown also in Fig.5a) measured at 10 different temperatures between 4.2 K and 9.05 K. (b) Calculations of the tunneling spectra versus temperatures performed with Eq.(1) in the frame of the the S_dIS_s convolution model. Γ_d , Γ_s , Δ_s values are normalized to $\Delta_d=1$.

$G(V)$ at 9.05 K (the critical temperature of Nb, $T/T_c = 1$). Then we calculate $G(V)$ at various temperatures $T/T_c < 1$, normalize them by the calculated curve at $T/T_c = 1$, and finally compare them with the experiments. The agreement between Figs. 10(a) and 10(b) is remarkable. This shows that one

is able to characterize the quasiparticle scattering rates at both interfaces (YBCO/Au and Au/Nb) and learn about the interface nature.

IV. CONCLUSIONS

In summary we measured temperature, magnetic field, and crystallographic orientation dependencies of the quasiparticle tunneling spectra of YBCO/Au/Nb junctions. As superconductivity gets suppressed in Nb by increasing either temperature or magnetic field the Nb coherence peaks get suppressed and the ZBCP gradually develops, while the total number of states is conserved. The measurements are consistent with formation of Andreev bound states at the YBCO/Au/Nb junction interfaces. Conductance measurements of these junctions offered the unique possibility to test both earlier proposed models of Andreev bound states assisted quasiparticle tunneling from one superconductor to another: the S_dIS_s convolution model and the series connection $S_dI + IS_s$ of two decoupled interfaces model, and to prove the validity of the first one in our case. In high contrast to Josephson tunneling, the conductance spectra are crystallographic orientation *insensitive*: independent whether the tunneling occurs in the (100), (110) or both (100) and (010) directions simultaneously, a pronounced ZBCP is always observed. It follows that in our case, while both Josephson tunneling and quasiparticle tunneling are able to distinguish between *s*-wave and a superconducting order parameter with nodes, only Josephson tunneling is able to distinguish between *d*-wave and other possible symmetries characterized by a sign change, like d_{xy} -wave, etc. This is of importance when investigating the symmetry of the order parameter in a new, presumably unconventional superconductor. The crystallographic orientation insensitivity of the quasiparticle spectra proves the junction interface is rough. On the other hand Josephson tunneling suggests that (110) junctions consist of alternating regions with positive and negative critical current densities. Furthermore, we have seen that by increasing the Au barrier thickness over a certain limit the ZBCP completely vanishes and therefore the signature of the *d*-wave is lost. In contrast, the Josephson tunneling channel is still observable and consistent with the *d*-wave symmetry. All these differences show that Cooper pair and quasiparticle tunneling are complementary tools of investigation.

ACKNOWLEDGMENTS

Discussions with Kurt Scharnberg are gratefully acknowledged. Support through the ESF PiShift program is acknowledged. The group at the University of Twente further acknowledges support from the Dutch FOM and NWO foundations. D. Doenitz acknowledges support from the Evangelisches Studienwerk e.V. Villigst.

REFERENCES

- [1] C.-R. Hu, Phys. Rev. Lett. **72**, 1526 (1994); J. Yang, and C.-R. Hu, Phys. Rev. B **50**, 16766 (1994);
- [2] Y. Tanaka and S. Kashiwaya, Phys. Rev. Lett. **74**, 3451 (1995); S. Kashiwaya and Y. Tanaka, Phys. Rev. B. **51**, 1350 (1995); S. Kashiwaya et al., Phys. Rev. B. **53**, 2667 (1996);
- [3] J.H. Xu, J.H. Miller, Jr., and C.S. Ting, Phys. Rev. B. **53**, 3604 (1996);
- [4] C.-R. Hu, Phys. Rev. B **57**, 1266 (1998);
- [5] S. Kashiwaya and Y. Tanaka, Rep. Prog. Phys. **63**, 1641 (2000).
- [6] T. Löfwander et al., Supercond. Sci. Technol. **14**, R53 (2001).
- [7] C.C. Tsuei and J.R. Kirtley, Rev. Mod. Phys. **72**, 969 (2001);
- [8] J. W. Ekin et al., Phys. Rev. B **56**, 13746 (1997); L. Alff et al., Phys. Rev. B **58**, 11197 (1998).
- [9] B. Chesca, M. Seifried, T. Dahm, N. Schopohl, D. Koelle, R. Kleiner, A. Tsukada, Phys. Rev. B **71**, 104504 (2005).
- [10] R. Wilkins, M. Amman, R.E. Soltis, E. Ben-Jacob, and R. C. Jaklevic, Phys. Rev. B **41**, 8904 (1990); J. R. Gavaler et al., Physica C **162- 164**, 1051 (1989).
- [11] M. Aprili, M. Covington, E. Paraoanu, B. Nidermeier, and L. H. Greene, Phys. Rev. B **57**, R8139 (1998);
- [12] M. Covington and L. H. Greene, Phys. Rev. B **62**, 12440 (2000).
- [13] H. J. H. Smilde et al., Appl. Phys. Lett. **80**, 4579 (2002).
- [14] H. J. H. Smilde, Ariando, D. H. A. Blank, G. J. Gerritsma, H. Hilgenkamp, and H. Rogalla Phys. Rev. Lett. **88**, 057004 (2002).
- [15] V. Ambegaokar and B.I. Halperin, Phys. Rev. Lett. **22**, 1364 (1969); C.M. Falco et al.,

Phys. Rev. B **10**, 1865 (1974).

[16] H. Hilgenkamp, J. Mannhart, and B. Mayer, Phys. Rev. B **53**, 14 586 (1996).

[17] R. G. Mints and V. G. Kogan, Phys. Rev. B **55**, R8682 (1997).

[18] Yu.S. Barash et al., Phys. Rev. B **55**, 15282 (1997).

[19] M. Fogelström et al., Phys. Rev. Lett. **79**, 281 (1997).

[20] R.C. Dynes and T.A. Fulton, Phys. Rev. B **3**, 3015 (1971).

[21] We mention here that similar results may well be obtained considering multiple facets with different orientations. The only difference is that in this case $J_c(x)$ varies in steps rather than continuously.